proceedings

MDPI

Type of the Paper (Abstract)

WTB-IRT: Modelling and Measurement of Thermal Contrast in wind turbine rotor blades (WTBs)†

Somsubhro Chaudhuri [1]*, Rainer Krankenhagen [1], Ivana Lapšanská [1], Michael Stamm [1]

[1] Bundesanstalt für Materialforschung und -prüfung (BAM), Berlin, Germany
* Correspondence: somsubhro.chaudhuri@bam.de
† Presented at the AITA 2025, Kobe Japan, 15-19 September 2025.

Abstract: The rapid growth of wind energy infrastructure over the past two to three decades has led to an urgent need for advanced non-destructive testing (NDT) methods—both for newly installed wind turbine blades (WTBs) and for ageing components nearing the end of their service life. Among emerging techniques, passive infrared thermography (IRT) offers a promising solution by enabling contactless, time-efficient inspection based on naturally occurring thermal variations. The effectiveness of passive IRT depends on the presence of sufficient thermal contrast to distinguish surface features, subsurface structures, and defects. To better understand the possibility of obtaining such contrast in composite structures such as WTBs, a controlled study was carried out on a blade section exposed to programmed temperature transients in a climate chamber. Infrared measurements were recorded, and the thermal behaviour of the specimen was simulated using finite element models (FEM) in COMSOL Multiphysics. Although direct validation is limited by measurement uncertainties and transient effects, the comparison provides insight into the capabilities and limitations of FEM in replicating real-world thermal behaviour. This paper focuses specifically on the challenges related to the modelling approach.

Keywords: Passive infrared thermography; wind turbine blades; non-destructive testing; NDT; finite element modelling; FEM; thermal contrast.

1. Introduction

Passive infrared thermography (IRT) offers the advantage of enabling ground-based inspections of operational WTBs with reduced turbine downtime compared to rope access methods. In addition, IRT can capture subsurface features [1]. The quality of such thermal inspections depends largely on the occurrence of thermal contrasts, which is influenced by both environmental conditions and the internal structure of the blade. The first reporting of IRT on WTB was in 2005 by Meinlschmidt and Aderhold, where they showed the detection of inner features in WTBs laying on the ground (i.e. unmounted), as well as on operational turbines [2]. The authors showed that both active as well as passive IRT could reveal interesting features, with the latter using boundary conditions such as solar irradiation and air temperature variations as sources of thermal excitation.

In operational setting, the appearance and disappearance of thermal contrasts on wind turbine rotor blade surfaces due to diurnal temperature changes remains insufficiently studied. The influencing factors include the environment conditions before and during a measurement, as well as the surface properties, inner structure and thermal properties of the WTB. Studies have been performed that attempted to incorporate these

Academic Editor: Firstname Lastname

Published: date

Citation: To be added by editorial staff during production.

variables into a finite element model (FEM) and validate it with experimental results [3, 4]. However, as complex environmental conditions are challenging to accurately reproduce in simulations, an experiment in a controlled environment such as a (large enough) climate chamber would be fitting. They are already used for calibration of IRT cameras [5]. Although there is evidence of WTBs being tested in climate chambers, no investigation of the evolution of thermal contrast was found in literature. Such controlled boundary conditions can be used as reliable input for FEM simulations, given that the geometry and structure of the WTB is known.

This paper briefly discusses the evaluation of a FEM simulation of a test performed in a climate chamber with controlled temperature transients, focussing on the challenges associated with modelling the various boundary conditions. The conference presentation includes results from the evaluation of thermal contrast.

2. Methodology

A section of a decommissioned WTB of an unknown manufacturer was investigated. Figure 1a shows the investigated suction side (SS) and Figure 1b the cross-section of the blade. Access to the cross-section enabled the design of a model for simulations in COMSOL Multiphysics, shown in Figure 1c. The specimen has also been investigated in a previous study performed with active thermography and under natural weather conditions [3]. The leading edge (LE) is covered with LE damage protection and the hollowed spaces were filled with crumpled paper to limit air exchange with the surroundings (imitating "closed WTB" i.e. the real-world).

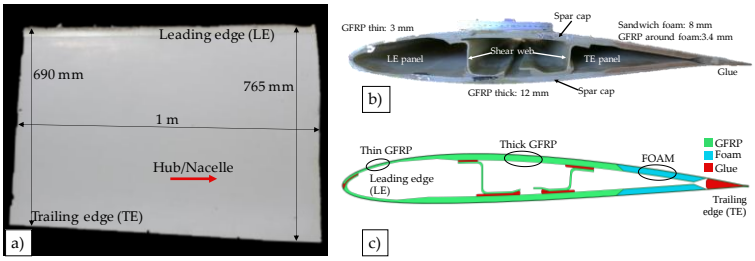

Figure 1. a) Suction side of WTB section investigated in a climate chamber; b) cross-section of the investigated specimen; c) FEM built in COMSOL Multiphysics using the cross-section.

The climate chamber is of dimensions 1800x6000x2000 mm equivalent to a volume of 21 m^3. The WTB section as well as the IRT camera are shown in Figure 2a. Figure 2b presents three separately measured temperature transients within the chamber, compared with the input program consisting of heating and cooling at 2 K/hour. Temperature sensor "therm_1" is used to regulate the air in the climate chamber, with "therm_2" (also seen in Figure 2a) measuring the air temperature closer to the specimen. The transient measured with "therm_2" was used as input for the FEM simulations. T_{slit}, obtained from the IRT measurements, represents the temperature of the interior wall of the chamber. The camera used is an InfraTec ImageIR 8800 with a cooled MCT sensor, a calibration range of -10 to 40 °C and NETD of <30 mK. Optics with a focal length of 25 mm and an integration time of 453 µs at 1 frame per second were used. The camera setting results in a spatial resolution of 1.5 mm/pixel.

The FEM was meshed with balanced data convergence and simulation time. Thermal processes were only simulated within a cross-section slice of the profile, but not along the original blade axis (horizontal in Fig.3a). Therefore, the simulated surface temperature was simply extracted along the horizontal axis in Fig. 3b) resulting in a regular striped pattern. This makes it considerably easier to compare the data graphically with the

thermogram. Thermal properties were consistent with previous work of the same specimen [3], with the primary difference being the convective heat transfer coefficient h applied to replicate the conditions in the climate chamber. h_{front} = 40 W/m²K was used for the side of the WTB section facing the camera and the chamber's fans, h_{rear} = 5 W/m²K for the rear side, and h_{inner} = 0 W/m²K for the inside of the blade. These values were derived from empirical relations for multiple large diameter impinging jets [6].

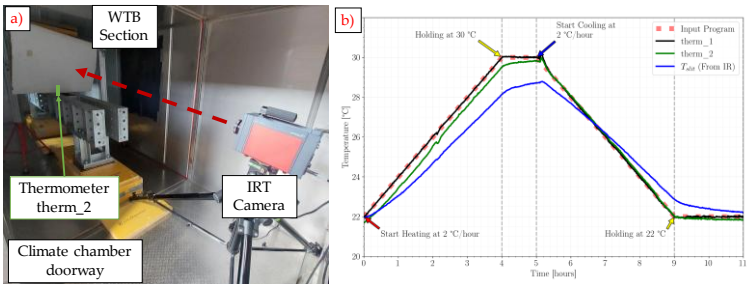

Figure 2. a) annotated photograph of WTB section within the climate chamber along with the IRT camera; b) Comparison of different temperature transients measured within the climate chamber: "Input Program" represents the input program defined for the climate chamber; "therm_1" is the air temperature directly at the fan that controls the chamber, "therm_2" is the air temperature nearby the specimen, T_{slit} is an estimated wall temperature observed by the IRT camera.

3. Results

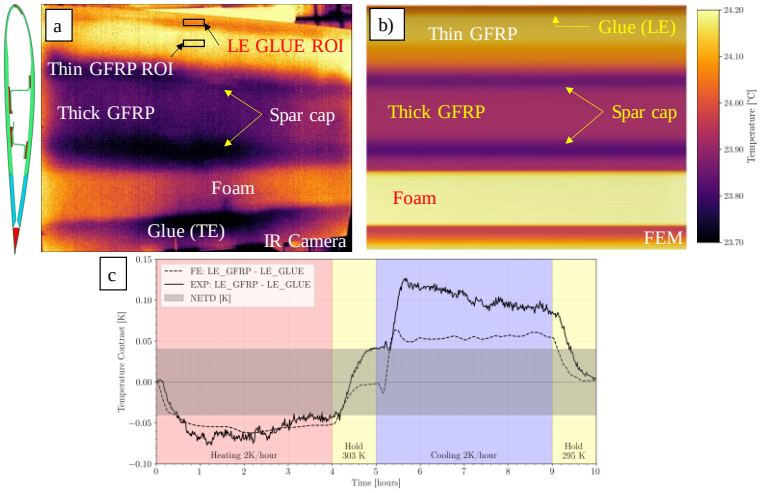

Figure 3. a) annotated thermogram after 85 minutes of heating at 2 K/hour; b) corresponding FEM simulation of the same time step; c) evolution of contrast between the LE GLUE ROI and thin GFRP ROI across the temperature transient shown in Figure 2b), the different cycles with heating up, holding and cooling as well as the NETD level are indicated by background coloring.

Figure 3a shows a thermogram after 85 minutes of heating at 2 K/hour. The foam section appears warmer compared to thick GFRP and glue due to its relatively higher thermal diffusivity, and thin GFRP appears warmer compared to thicker GFRP due to difference in material thickness. The spar cap warms slower than the surrounding thick GFRP as there is more material with more heat capacity to absorb the heat (the glue attaching the shear web to the spar cap). FEM simulations also accurately capture these thermal contrasts (Figure 3b), apart from some inhomogeneous features in the blade (foam irregularity in Figure 3a below the "Foam" annotation") that were not modelled in the simulation. It is important to highlight that the FEM does not capture the tapered chord length (distance between LE and TE), as explained above. In Figure 3c, the evolution of

the thermal contrast between the LE Glue and the thin GFRP (also at LE; both ROIs are visible in Figure 3a) is shown for the entire measurement period. During the heating, the simulation shows good agreement with the experimental data, and the contrast exceeds the NETD of the IR camera, and thus can be deemed to be detectable. However, during the hold phase (at 303 K), a stark deviation occurs between the FEM and experimental data, which continues into the cooling phase. This may be attributed to spatial inhomogeneity of the climate chamber during the heating and cooling transitions, which is not part of the model as the transient temperature used as input is in only one location, i.e. near the TE (see Figure 2a). The outcome of the conducted experiment and corresponding simulation indicates that LE contrast can be detected thermographically in the absence of solar irradiation only when the air temperature changes by least 2 K/h for a sustained period of 15 minutes or more. This contrast however holds as long as the temperature keeps rising or falling which indicates large time windows for thermographic inspections of operational WTBs. This conclusion is specific to the geometry of the LE glue joint investigated.

4. Conclusions

This study aimed to validate a thermal FEM of a wind turbine blade (WTB) section using a simplified climate chamber experiment. The specimen underwent a symmetric heating–cooling cycle, with surface temperatures recorded using infrared thermography. Model validation included comparisons of thermograms, transients, profile lines, and thermal contrast at an internal feature. The FEM simulation accurately captured surface temperature evolution, with deviations limited to 0.1–0.2 K over a 2K/hour transient over 4 hours. These differences stemmed from unmodelled boundary effects. The simulation reliably predicted thermal contrast development at the leading-edge bond under overcast conditions (as no solar irradiation was implemented or modelled). Future work will extend the model to account for sun, wind, and clear-sky scenarios.

Author Contributions: Somsubhro Chaudhuri: Methodology, Software, Hardware, Data curation, Inspection, FEM, Validation, Formal analysis, Writing, Visualisation. **Rainer Krankenhagen**: Conceptualisation, FEM, data curation, validation, writing, visualisation. **Ivana Lapšanská**: Hardware, Inspection, Data curation, Writing – reviewing & editing. **Michael Stamm**: Visualisation, Writing – reviewing and editing.

Acknowledgments: The authors would like to thank the staff from BAM 7.2 for their assistance in using their climate chamber, specifically Mr. Patrick Simon and Dr. Ing. Marc Thiele.

Conflicts of Interest: The authors declare no conflict of interest.

References

1. Vollmer, M. and K.P. Möllmann, *Infrared Thermal Imaging: Fundamentals, Research and Applications*. 2018: Wiley DOI: 10.1002/9783527693306.
2. Meinlschmidt, P. and J. Aderhold. *Thermographic Inspection of Rotor Blades*. in *9. ECNDT 2006*. 2006. Berlin (Germany).
3. Chaudhuri, S., M. Stamm, and R. Krankenhagen *Weather-dependent passive thermography and thermal simulation of in-service wind turbine blades*. Journal of Physics: Conference Series, 2023. **2507**, 012025 DOI: 10.1088/1742-6596/2507/1/012025.
4. Worzewski, T., et al. *Thermographic inspection of a wind turbine rotor blade segment utilizing natural conditions as excitation source, Part I: Solar excitation for detecting deep structures in GFRP*. Infrared Physics & Technology, 2016. **76**, 756-766 DOI: http://dx.doi.org/10.1016/j.infrared.2016.04.011.
5. Brazane, S., et al., *Management of thermal drift of bolometric infrared cameras: limits and recommendations.* Quantitative InfraRed Thermography Journal, 2025. **22**(1): p. 54-69 DOI: 10.1080/17686733.2023.2290304.
6. Zuckerman, N. and N. Lior, *Jet Impingement Heat Transfer: Physics, Correlations, and Numerical Modeling*, in *Advances in Heat Transfer*, G.A. Greene, et al., Editors. 2006, Elsevier. p. 565-631.